
COLLABORATIVE BROADCAST IN $\mathcal{O}(\log \log n)$ ROUNDS

A PREPRINT

Christian Schindelhauer
 University of Freiburg,
 George-Köhler-Allee 51,
 79110 Freiburg im Breisgau, Germany
 schindel@tf.uni-freiburg.de

Aditya Oak **Technical University of Darmstadt,**
 Hochschulstraße 10,
 64289 Darmstadt, Germany
 oak@st.informatik.tu-darmstadt.de

Thomas Janson
 University of Freiburg,
 George-Köhler-Allee 51,
 79110 Freiburg im Breisgau, Germany
 thomas@janson-online.de

June 11, 2019

ABSTRACT

We consider the multihop broadcasting problem for n nodes placed uniformly at random in a disk and investigate the number of hops required to transmit a signal from the central node to all other nodes under three communication models: Unit-Disk-Graph (UDG), Signal-to-Noise-Ratio (SNR), and the wave superposition model of multiple input/single output (MISO).

In the MISO model, informed nodes cooperate to produce a stronger superposed signal. We do not consider the problem of transmitting a full message nor do we consider interference. In each round, the informed senders try to deliver to other nodes the required signal strength such that the received signal can be distinguished from the noise.

We assume either sufficiently high node density $\rho = \Omega(\log n)$ or some $\Omega(\log n)$ initially informed nodes uniformly distributed with $\rho = \Omega(1)$ in order to launch the broadcasting process. In the unit-disk graph model, broadcasting needs $\mathcal{O}(\sqrt{n/\rho})$ rounds. In the other models, we use an Expanding Disk Broadcasting Algorithm, where in a round only triggered nodes within a certain distance from the initiator node contribute to the broadcasting operation.

This algorithm achieves a broadcast in only $\mathcal{O}\left(\frac{\log n}{\log \rho}\right)$ rounds in the SNR-model. Adapted to the MISO model, it broadcasts within $\mathcal{O}(\log \log n - \log \log \rho)$ rounds. All bounds are asymptotically tight and hold with high probability, i.e. $1 - n^{-\mathcal{O}(1)}$.

1 Introduction

Understanding the limits of multi hop communications and broadcasting is important for the development of new technologies in the wireless communication sector. In the recent decades, ever more realistic models for the communication have been considered. First, graph models have been considered to describe the communication between wireless communication nodes, resulting in the Radio Broadcast model [1]. However, this model neglects the communication range, which has led to a geometric graph model, the Unit-Disk Graph (UDG) [2], which we also consider here. It is based on the observation that there is path loss of the sender energy with increasing distance between the sender and the receiver. In order to distinguish the signal from the noise, the signal to noise energy ratio (SNR) has to be above certain threshold, which leads to the disk shaped model for radio coverage.

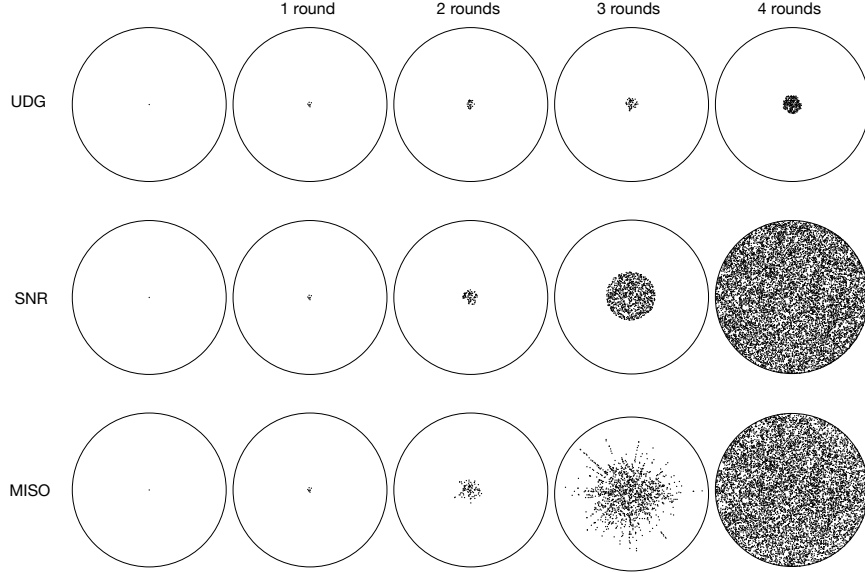


Figure 1: Four rounds of repeated collaborative broadcast in the UDG, SNR, and MISO model for 10,000 senders randomly distributed in a disk with radius 30 and wavelength $\lambda = 0.1$

However, if one carefully models the influence of the noise on the SNR, one sees that interference-free communication links inside a disk are still possible because of the polynomial nature of the energy path loss. This model is known as the SINR-model [3]. This, however, is still far from reality, where one sees a superposition of electromagnetic waves, which can be expressed by the addition of the complex Fourier coefficients. In this model, diversity gain and energy gain [4] enable higher bandwidth and higher communication range. There is a trade-off between these two features and certain properties of the number of coordinated senders, receivers and the channel matrix have to be met. However, one sees that in practice this one-hop communication has already led to better networking solutions.

For our theoretical analysis, we concentrate on an open space model with no interfering communications. We want to find the theoretical limitations of a collaborative multi-hop broadcast. For this, we are interested in sending a signal which contains no information. This signal is sent by the sender node positioned at the center of a disk in which all other nodes are randomly distributed. Thus, in the first round the first sender activates some small number of neighboring nodes. Then, in every subsequent round, all of them try to extend the set of informed nodes as far as possible, who then join in the next round, until all nodes of the disk are informed (or the process cannot reach any further nodes).

2 Related Work

Broadcasting algorithms have been widely optimized for speed, throughput, and energy consumption. A lot of algorithms apply MAC (medium access) protocols like TDMA (Time Division Multiple Access)[2, 5, 6, 7], CDMA (Code Division Multiple Access) [8, 9], FDMA (Frequency Division Multiple Access) [9] to increase spatial reuse. Physical models with high path loss exponent $\alpha > 2$ are beneficial here and increase the spatial reuse with only local interference. With spatial reuse, parallel point-to-point communications are possible which either spread the same broadcast message in the network or pipeline multiple broadcast messages at the same time. The latter can achieve a constant broadcasting rate for path loss exponent $\alpha > 2$. Cooperative transmission with MISO (Multiple Input Multiple Output) is applied to increase the transmission range and increase the broadcast speed by a constant factor (where underlying MAC protocols still work).

Here, we focus on broadcast speed and allow as many as possible nodes cooperate in transmitting the same broadcast message with MISO. The obvious tradeoff here is broadcast speed against broadcast rate, since pipelining and spatial reuse is limited.

Broadcasting has been first considered for a graph based model, where interference prevents communication and a choice has to be made which link should be used for propagation. Since we do not consider interference and allow the usage of all links a simple flooding algorithm achieves the optimal bound of the diameter of the network. So, these works (see [1] for a survey) do not apply here. However, even if interference is considered there is only a constant factor

slow down in the Unit-Disk-Graph model [5]. Note that Unit-Disk-Graphs are connected, when the node density of the randomly placed nodes is large enough [10].

Launched by the seminal paper of [11] the SNR (Signal to Noise Ratio) model has gained a lot of interest. Here, signals can be received if the energy of the sending nodes is a constant factor larger than the sum of noise energy and interference. This model leads to a smooth receiver area with near convexity properties [12].

When the energy of each sender is constrained, in [6] it is shown that the SNR-model does not give much improvement compared to the UDG-model. So, [6] incorporates the unit disk model with the SINR (Signal to Interference and Noise) model. The focus are TDMA scheduling schemes to enhance the network capacity. The path-loss exponent in the SINR model is chosen with $\alpha > 2$ and interference has only local effects for unsynchronized transmitters. In this context, the SNR model is used for each sender separately. So, the problem of broadcast mainly reduces to range assignment and scheduling problem, for which the number of rounds approaches the diameter [7].

For the superposition model the problem of point-to-point communication has been considered mostly for beam-forming for senders (MISO) or receivers (SIMO — Single Input Multiple Output). For MIMO (Multiple Input Multiple Output), most of the research is concerned with the energy gain and diversity gain, as well as the trade-off. For an excellent survey we refer to [4]. Besides the standard approach, where sender antennas and receiver antennas are connected to one device and only a one hop communication is considered, there is also a lot of research in independent senders and receivers.

A transmission with cooperative beamforming requires phase synchronization of the collaborating transmitters to produce a beam and sharing the data to transmit. The authors of [13] present therefore a two phase scheme: in phase one, the message is spread among nodes in a disk in the plane around the node holding the original message. The open-loop and closed-loop approach can be used to synchronize nodes with synchronization to the destination or a known node position and time synchronization. In phase two, the synchronized nodes transmit jointly the message towards the destination.

For the MIMO model in [14] and [15] the authors give a recursive construction, which allows a capacity of n for n senders using MIMO communication. However, in [16] an upper bound of \sqrt{n} has been proved. This seeming contradiction has been addressed in [17], where they address the question whether distributed MIMO provide significant capacity gain over traditional multi-hop in large ad hoc networks with n source-destination pairs randomly distributed over an area A . It turns out that the capacity depends on the ratio \sqrt{A}/λ , it describes the spatial degree of freedom. If it is larger than n it allows n degrees of freedom [14]. If it is less than \sqrt{n} the bound of [16] holds. For all regimes optimal constructions are given in these papers. While in [14] path loss exponents $\alpha \in (2, 3]$ are considered, for $\alpha > 3$ the regularity of the node placement must be taken into account [15].

While this research is largely concerned with the diversity gain, we study the physical limitations of the energy gain. In [18, 19] a method is presented to amplify the signal by using spatially distributed nodes. They explore the trade-off between energy efficiency and spectral efficiency with respect to network size. In [20] a distributed algorithm is presented which produced a growing beam by adding more and more senders.

In [21] the asymptotic behavior of the rounds for a unicast has been analyzed in great detail and an upper and lower bound of $\Theta(\log \log n)$ rounds has been proven. If the nodes are placed on the line it takes an exponential number of rounds [22]. The generalization of these observations for different path loss models can be found in [23]. In [24] it is shown that the sum of all cooperating sender power can be reduced to the order of one sender, while maintaining a logarithmic number of rounds to send a message over an n hop distance.

A practical approach already uses this technology. Glossy [8] is a network architecture for time synchronization and broadcast including the network protocol for flooding, integration in network protocols of the application, and implementation in real-world sensor nodes. If multiple nodes transmit the same packet in a local area, the same symbol of the different transmitters will overlap at a receiver without inter-symbol interference if the synchronization is sufficient. The superposed signals of the same message have random phase shifts and in the expectation add up constructively. Faraway out of sync transmitters produce noise-like interference the influence of which is alleviated at the receiver via pseudo-noise codes. While a high node density increases interference in common network protocols, a higher density is beneficial here and increases the transmission range and reduces the number of broadcasting rounds.

Glossy is the underlying technology for the so-called Low-Power Wireless Bus [25], where this multi-hop broadcast allows to flood the network with a broadcasting message. The energy efficiency was further improved in Zippy [26], which is an on-demand flooding technique providing robust wake-up in the network. Unlike Glossy, Zippy uses an asynchronous wake-up flooding. In [27] the problem of Rayleigh fading for synchronized identical signals is addressed by producing a low frequency wake-up signal, which results from the beat frequency of closely chosen frequencies. This allows the usage of a passive receiver technology.

In [9] a multistage cooperative broadcast algorithm is proposed similar to our work. Likewise here, nodes are uniformly distributed in a disk. A continuum approximation is used to approximate the behavior of the disk with high node density. A minimum SNR threshold is assumed for successful reception of the message. The algorithm works in stages, in the first stage, node at the center of the disk transmits message. All nodes which receive this message are considered as level 1. In the next stage, level 1 nodes re-transmit the message in this way set of informed nodes keeps growing in radially outward direction. Nodes belonging to same levels form concentric rings. Source node emits single block of data. In [28], the authors consider a similar problem and a similar algorithm. They also consider source node transmitting a continuous message signal. Initially source node which is at the center of the disk, transmits the message signal. In the next round, level 1, i.e. the set of nodes that received the message in the previous round, transmits the message signal which is received by next level and the source node does not transmit message. In the next round, the source transmits the next message block. In this way, levels send and receive the message block in alternate rounds. In our work, we consider that in each round, all informed nodes send a single message cooperatively.

The authors of [29] consider a system model similar to our work. They use two phase opportunistic broadcasting to achieve linear increase in propagation distance. In phase 1, nodes inside a disk of specific radius broadcast message with different random phases while in phase 2, a node broadcasts the message to its neighboring nodes. These phases are performed repeatedly to broadcast the message. Improving on this work we obtain better bounds by coordinating the phase of the nodes, while we consider only the path loss factor of $\alpha = 2$.

To our knowledge no research has considered the asymptotic number of rounds to cover the disk using cooperative broadcast, which is the main focus of this work. While [8, 25, 26, 27] use only simulation and [9, 28, 29] prove all their statements only for the expectation in the continuum limit, i.e. when the number of nodes approaches infinity. Our results are to our knowledge the first asymptotic results in MISO that hold for a finite number of nodes n with high probability, i.e. $1 - n^{-O(1)}$.

3 The Models

We assume n nodes $v_1, \dots, v_n \in \mathbb{R}^2$ uniformly distributed in a disk of radius R centered at origin, where the additional node v_0 resides. The density is denoted by $\rho = n/(\pi R^2)$. Each node knows the disk radius R , its location and all nodes are perfectly synchronized.

We say that a node is triggered or informed, when it has received a signal carrying no further information. The objective is to send the broadcast signal from the center node v_0 to all other nodes where in each round the set of sending nodes is increased by the triggered nodes of the last round.

We concentrate on generating a signal and leave the problem sending a full message to subsequent work. The signal is a sinus wave with wavelength λ . We normalize the speed of light as $c = 1$ by choosing adequate units for time and space. In our theoretical framework we assume that every node knows its exact position in the plane, is synchronized (well enough in order emit phase-coordinated signals) and is able to precisely emit the signal at a given point in time with a certain phase shift and a fixed amplitude.

We consider three communication models in our analysis: Unit-Disk-Graph (UDG) in Chapter 4, the Signal-to-Noise Ratio (SNR) of uncoordinated nodes in Chapters 5 and 6, and Multiple Input/Single Output (MISO) for coordinated senders in Chapter 7.

3.1 The MISO Model

The coordination of nodes refers here to synchronized signals allowing a radiation pattern containing strong beams, i.e. a beamforming gain. Many physical properties are covered in the **Multiple Input/Single Output (MISO)** model based on superposition of waves. Every node can serve either as sender or as receiver. A node can demodulate a received signal $rx(t) \in \mathbb{C}$ if the square of the length of the Fourier coefficient over an interval of $\delta \gg \lambda$ is larger than β , i.e.

$$z = \frac{1}{\delta} \int_{t=t_0}^{t_0+\delta} rx(t) e^{-i2\pi t/\lambda} dt \quad (1)$$

$$|z|^2/N_0 \geq \beta \quad (2)$$

with imaginary number $i = \sqrt{-1}$ and t denotes time. In this notation we have normalized the energy with respect to the time period and assume δ , N_0 and β as constants. Inequality 2 demands that the signal-to-noise energy ratio is large enough to allow a successful signal receptions, i.e. $\text{SNR} \geq \beta$ for signal power $|z|^2$ and additive white noise with power N_0 over time δ .

Each sending node $j \in \{1, \dots, n\}$ can start sending at a designated time t_1 and stops at t_2 , described by the function

$$s_j(t) = \begin{cases} a \cdot e^{i2\pi(t-t_1)/\lambda}, & t \in [t_1, t_2] \\ 0, & \text{otherwise} \end{cases} \quad (3)$$

where $a \in \mathbb{C}$ may encode some signal information, e.g. via Quadrature Amplitude Modulation (QAM). Since we are only interested in transmitting a single signal we choose $a = 1$ or $a = e^{i\varphi}$, when we use a phase shift φ . The total signal received at a node $q \in \mathbb{R}^2$ is modeled by

$$\text{rx}(t) = \sum_{j=1}^n \frac{s_j(t - \|q - v_j\|_2)}{\|q - v_j\|_2}, \quad (4)$$

which models the free space transmission model with a path loss factor of two for the logarithm of sender and receiver energy. We are aware, that this equation describes only the far-field behavior, which starts at some constant numbers $c_f > 1$ of wavelengths, i.e. $\|q - v_i\|_2 \geq c_f \lambda$ (Antennas have unit size and are neglected in this equation). Hence, every time $\|r - v_i\|_2 < c_f \lambda$, we will replace the denominator $\|q - v_i\|_2$ by $c_f \lambda$ in this expression. We assume that $c_f \lambda \leq 1$ and therefore $\lambda < 1$.

3.2 Unit Disk Graph Model

For nodes v_1, \dots, v_n the geometric **Unit Disk Graph** is defined by the set of edges (v_i, v_j) where the nodes have at most $\|v_i, v_j\|_2 \leq 1$. In each round a message or signal can be moved from a node to an adjacent node. So, collaborative sending is simply ignored. Yet, also ignore the negative effect of interference is ignored. In this model messages can be sent along edge in parallel, independently from what happens somewhere else.

The following Lemma shows the strong relationship between the single sender MISO model and the UDG model.

Lemma 1. *If only one sender u sends a signal in the MISO model with amplitude $a \in \mathbb{R}^+$, then a node v in distance d receives it if and only if $d \leq \frac{a}{\sqrt{\beta N_0}}$.*

Proof. In the MISO model the sender produces the signal $s_j(t) = a e^{i2\pi t/\lambda + i\phi}$ for $t \in [0, T]$ for some sending time T and phase shift ϕ and otherwise $s_j(t) = 0$. For distance d the received signal is

$$\text{rx}(t) = \frac{s_j(t-d)}{d} = \frac{a e^{i2\pi(t-d)/\lambda + i\phi}}{d},$$

if $t \in [d, T+d]$ and otherwise $\text{rx}(t) = 0$. Therefore for $\delta = T$:

$$\begin{aligned} z &= \frac{1}{T} \int_{t=d}^{d+T} \text{rx}(t) e^{-i2\pi t/\lambda} dt \\ &= \frac{1}{T} \int_{t=d}^{d+T} \frac{a e^{i2\pi(t-d)/\lambda + i\phi}}{d} e^{-i2\pi t/\lambda} dt \\ &= \frac{1}{T} \int_{t=d}^{d+T} \frac{a e^{-i2\pi d/\lambda + i\phi}}{d} dt \\ &= \frac{a}{d} e^{-i2\pi d/\lambda + i\phi} \end{aligned}$$

Now $|z| = a/d$ and therefore if $|z|^2 = \frac{a^2}{d^2} \geq \beta N_0$ then u can receive the signal. \square

This Lemma implies that if $a^2 = \beta N_0$, then the MISO model is equivalent to the Unit-Disk Graph (UDG) model with sending radius 1, if only one sender is active. In order to compare these two models fairly, we fix $a = 1$ and set $\beta N_0 = 1$.

3.3 The Signal-to-Noise-Ratio Model

The **Signal-to-Noise-Ratio (SNR)** model adds the received signal energy of all senders, i.e. a signal is received at q in the SNR model, if for sender energy $S_j := a_j^2$, where a_j denotes the amplitude of sender v_j we have for

$$RS := \sum_{j=1}^n \frac{S_j}{(\|q - v_j\|_2)^2}$$

that the signal to noise ratio is large enough, i.e.

$$\frac{RS}{N_0} \geq \beta.$$

If we assume that the senders' starting time is not coordinated but independently chosen at random, then we the following Lemma shows that

$$\mathbb{E}[|z|^2] = \sum_{j=1}^n \frac{a_j^2}{(\|q - v_j\|_2)^2}.$$

Lemma 2. *At the receiver q the expected signal energy S of senders v_1, \dots, v_n with random phase shift ϕ_i and amplitude a_i in the MISO model is*

$$\mathbb{E}[S] = RS = \sum_{j=1}^n \frac{a_j^2}{(\|q - v_j\|_2)^2}.$$

Proof. We assume that at the receiver q senders have started sending such that the sending time intervals $[t_j, t'_j]$ of sender v_j covers the time interval $[T, T + \delta]$ at q , i.e. $t_j + \|q - v_j\|_2 \leq t$ and $t'_j \|q - v_j\|_2 \leq t + \delta$. Each sender sends the signal $s_j(t) = a_j e^{i2\pi t/\lambda + i\phi_j}$ in interval $[t_j, t'_j]$ with random phase shift ϕ_j . The received signal at q during $t \in [T, T + \delta]$ is by definition:

$$\begin{aligned} \text{rx}(t) &= \sum_{j=1}^n \frac{s_j(t - \|q - v_j\|_2)}{\|q - v_j\|_2} \\ &= \sum_{j=1}^n \frac{a_j}{\|q - v_j\|_2} e^{i2\pi(t - \|q - v_j\|_2)/\lambda + i\phi_j}. \end{aligned}$$

So, the received signal z is:

$$\begin{aligned} z &= \frac{1}{\delta} \int_{t=t_0}^{t_0+\delta} \text{rx}(t) e^{-i2\pi t/\lambda} dt \\ &= \frac{1}{\delta} \int_{t=t_0}^{t_0+\delta} \sum_{j=1}^n \frac{a_j}{\|q - v_j\|_2} e^{i2\pi(t - \|q - v_j\|_2)/\lambda + i\phi_j} e^{-i2\pi t/\lambda} dt \\ &= \frac{1}{\delta} \int_{t=t_0}^{t_0+\delta} \sum_{j=1}^n \frac{a_j}{\|q - v_j\|_2} e^{-i2\pi\|q - v_j\|_2/\lambda + i\phi_j} dt \\ &= \sum_{j=1}^n \frac{a_j}{\|q - v_j\|_2} e^{-i2\pi\|q - v_j\|_2/\lambda + i\phi_j} \\ &= \sum_{j=1}^n b_j e^{i\sigma_j}, \end{aligned}$$

where we substitute $b_j = \frac{a_j}{\|q-v_j\|_2}$ and $\sigma_j = -2\pi\|q-v_j\|_2/\lambda + \phi_j \bmod 2\pi$. Note that $\sigma_1, \dots, \sigma_n$ are again independent random variables and uniform distributed over $[0, 2\pi]$. Now, we observe.

$$\begin{aligned} \mathbb{E} \left[\left| \sum_{j=1}^n b_j e^{i\sigma_j} \right|^2 \right] &= \mathbb{E} \left[\left(\sum_{j=1}^n b_j e^{i\sigma_j} \right) \cdot \left(\sum_{j=1}^n b_j e^{-i\sigma_j} \right) \right] \\ &= \mathbb{E} \left[\sum_{j,k \in \{1, \dots, n\}} b_j b_k e^{i(\sigma_j - \sigma_k)} \right] \\ &= \sum_{j,k \in \{1, \dots, n\}} b_j b_k \mathbb{E} \left[e^{i(\sigma_j - \sigma_k)} \right] \\ &= \sum_{j \in \{1, \dots, n\}} b_j^2 \mathbb{E} \left[e^{i(\sigma_j - \sigma_j)} \right] + \sum_{j,k \in \{1, \dots, n\}, j \neq k} b_j b_k \mathbb{E} \left[e^{i\sigma_j} \right] \mathbb{E} \left[e^{-i\sigma_k} \right] \\ &= \sum_{j,k \in \{1, \dots, n\}} b_j^2, \end{aligned}$$

where we use that σ_j and σ_k are independent and that $\mathbb{E} [e^{i\sigma_j}] = 0$ because σ_j is uniform over $[0, 2\pi]$. Therefore $\mathbb{E} [|z|^2] = \sum_{j=1}^n \frac{a_j^2}{(\|q-v_j\|_2)^2}$. \square

This proof can also be found in [30]. Unlike in the coordinated MISO model, in the SNR model signals are sent with random phasing which induces a more regular radiation pattern.

Under the assumption that $\mathbb{E} [|z|^2] / N_0 \geq \beta$ induces a successful reception, $a_j = 1$ and $\beta N_0 = 1$ we derive the Signal-to-Noise Ratio (SNR) model, where the energy of the uncorrelated received signals add up. Again, this model reduces to the UDG model if only one node is sending.

4 UDG Coverage

Let $\rho = \frac{n}{\pi R^2}$ denote the density of nodes. The probability that $n-1$ nodes are not in a given area of size $\pi/8$ is

$$\left(1 - \frac{\pi/8}{\pi R^2}\right)^{n-1} = \left(1 - \frac{\rho\pi}{8n}\right)^{n-1} \leq \exp\left(-\left(1 - \frac{1}{n}\right)\frac{\rho\pi}{8}\right),$$

which is less than $1/n^c$ for $\rho \geq \frac{8}{\pi}c \ln(n+1)$ for any $c > 1$ and $n \geq 2$. Now, consider six equally sized sectors of a unit disk around a node; there is at least a node with probability $1 - n^{-c+1}$.

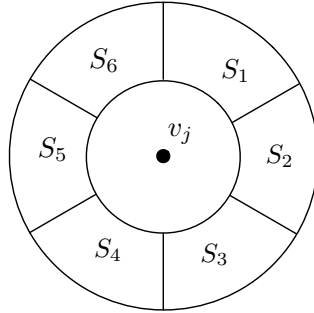


Figure 2: For a disk with radius 1 and area π and node density $\rho = \Omega(\log n)$, each of the sectors S_1, \dots, S_6 around a disk with area $\pi/8$ and sender v_j in the center are not empty with high probability

From this, it follows that UDG is connected (see [10] for a better bound) and that the diameter of the UDG is at most $8R = \mathcal{O}\left(\sqrt{n/\rho}\right)$.

Lemma 3. For $\rho = \Omega(\log n)$ in the UDG model, broadcasting needs $\mathcal{O}(\sqrt{n/\rho})$ rounds to inform all nodes with high probability.

Proof. Consider two nodes r_j and r_k with distance $d \geq R$. We have seen that each sector S_i contains at least a node with high probability. Now we route starting from r_j along the line L connecting r_j and r_k by choosing a node from a sector which is closer to r_k in a sector which in a corridor of width 2 around L . We pick a node from this sector and observe that the route advances at least $\frac{1}{4}$ in the direction towards r_k .

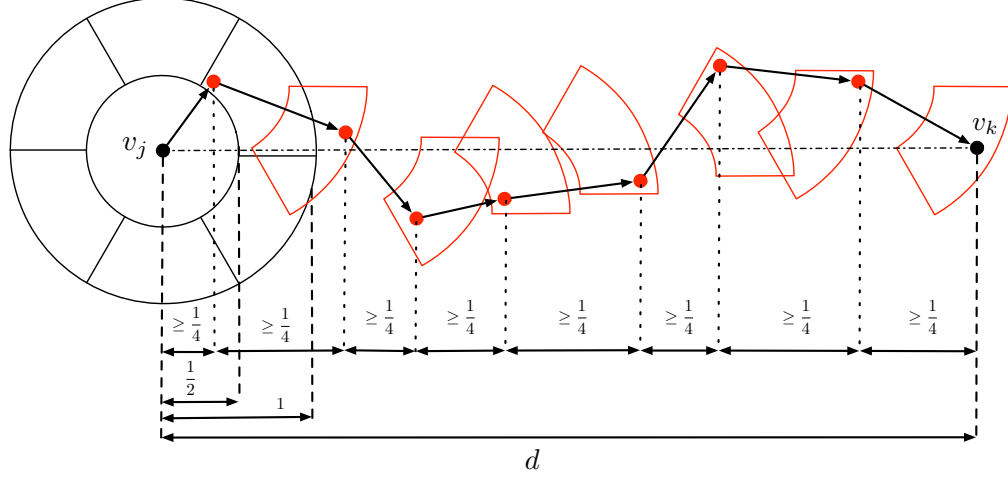


Figure 3: Routing from v_j to v_k using the unit-disk graph and non-empty sectors.

So, it takes at most $4R$ hops, where $R^2 = \frac{n}{\pi\rho}$. □

5 A Lower Bound for SNR Collaborative Broadcasting

The expected number of nodes $n(r)$ in a disk of radius r around the origin is sharply concentrated around the expectation $\rho\pi r^2$, if this value is larger than $\omega(\log n)$.

Lemma 4. For n randomly distributed nodes in a disk of radius R and a given smaller disk of radius r within this disk, let $n(r)$ denote the number of nodes there within. Then we observe:

$$\mathbb{E}[n(r)] = \pi\rho r^2, \quad (5)$$

$$\text{Prob}[n(r) \geq (1+c)\mathbb{E}[n(r)]] \leq e^{-\frac{1}{3}\min\{c, c^2\}\pi\rho r^2}. \quad (6)$$

Proof. We can reformulate $n(r)$ as the sum of the independent Bernoulli variables X_i , which denote $X_i = 1$ when node i falls into the smaller disk of radius r , and otherwise $X_i = 0$. We have $\text{Prob}[X_i = 1] = \frac{\pi r^2}{\pi R^2} = \frac{r^2}{R^2}$ and thus the expectation of $n(r)$ is the following.

$$\mathbb{E}[n(r)] = \mathbb{E}\left[\sum_{i=1}^n X_i\right] = n \frac{r^2}{R^2} = \frac{\pi\rho n r^2}{n} = \pi\rho r^2,$$

using $\rho = \frac{n}{\pi R^2}$. The other inequality follow by applying Chernoff bounds to $n(r)$. □

Theorem 1. For $\pi\rho \geq 1$ and $\rho = o(n)$ in the SNR-model at least $\Omega\left(\frac{\log n}{\max\{1, \log \rho\}}\right)$ rounds are necessary to broadcast the signal to all n nodes with high probability.

Proof. We start with the center node in the middle of the disk and denote by r_i the maximum distance of an informed node from the center of the disk. Let n_i denote the number of informed nodes in round i . By definition $r_0 = 0$ and $n_0 = 1$. Then, in round 1 we have $r_1 = 1$ by applying the SNR model for one sender.

We consider two cases.

1. Case: $\pi\rho \geq k \log n$.

Then, the expected number of nodes n_1 is $\pi\rho$ by Lemma 4 and for $\pi\rho \geq 1$ it is bounded as $n_1 \leq 2\pi\rho$ with high probability by choosing $c = 3k$.

Consider a receiver in distance d and assume for the lower bound argument that all nodes $n(r_i)$ in radius r_i send the signal. Since $\pi\rho r_i^2 \geq k \log n$ we have $n(r_i) \geq \frac{1}{2}\pi\rho^2$ with high probability. So, for $d \geq 4\sqrt{\rho}r$ and $\rho \geq 1$ we have

$$d - r \geq 4\sqrt{\rho}r - r \geq (4\sqrt{\rho} - 1)r \geq (4\sqrt{\rho} - \sqrt{\rho})r \geq 3\sqrt{\rho}r > \sqrt{2\pi\rho}r.$$

Then, the received energy is at most $\frac{n(r)}{(d-r)^2}$ where

$$\frac{n(r)}{(d-r)^2} < \frac{n(r)}{2\pi\rho r^2} \leq \frac{2\pi\rho r^2}{2\pi\rho r^2} \leq 1,$$

with high probability. So, no node farther than $r_{i+1} = 4\sqrt{\rho}r_i$ is informed in the SNR model in round i .

By induction after t rounds only nodes in distance of at most $r_t = (4\sqrt{\rho})^t$ can be informed, which only can inform all nodes in the disk of radius $R = \frac{n}{\pi\rho}$ if

$$(4\sqrt{\rho})^t \geq R = \frac{n}{\pi\rho},$$

yielding $t \geq \frac{\log n - \log \pi - \log \rho}{2 + \frac{1}{2} \log \rho} = \Omega\left(\frac{\log n}{\max\{1, \log \rho\}}\right)$ if $\rho = o(n)$ and $\rho \geq 1$.

2. $\pi\rho \geq 1$ and $\pi\rho \leq k \log n$.

For the proof we have to overcome the difficulty that the number of nodes in the unit disk may be too small to ensure high probability. We resolve this problem by overestimating the first radius $r_1 = \sqrt{\frac{k}{\pi\rho} \ln n}$. Then, the expected number of nodes in this disk is $n(r_1) = \pi\rho r_1^2 = 3k \ln n$ and $n(r_1) \geq 2\mathbb{E}[n(r_1)]$ with small probability, i.e. $1/n^k$.

Like in the first case we assume that in round r_i all nodes in this radius send. So, for $d \geq 4\sqrt{\rho}r$ and $\rho \geq 1$ the received energy is less than 1 within a distance of at most $r_{i+1} = 4\sqrt{\rho}r_i$.

Now the recursion is

$$r_t = (4\sqrt{\rho})^{t-1}r_1 = (4\sqrt{\rho})^{t-1}\sqrt{\frac{k}{\pi\rho} \ln n} = 4(4\sqrt{\rho})^{t-2}\sqrt{\frac{k}{\pi} \ln n}.$$

After t rounds nodes in distance of at most r_t can be informed, which can inform all nodes in the disk of radius $R = \frac{n}{\pi\rho}$ if

$$4(4\sqrt{\rho})^{t-2}\sqrt{\frac{k}{\pi} \ln n} \geq R = \frac{n}{\pi\rho},$$

yielding

$$t \geq 2 + \frac{\log n - \frac{1}{2} \log \log n - \frac{1}{2} \log \pi - \log \rho + \log k + 2}{2 + \frac{1}{2} \log \rho} = \Omega\left(\frac{\log n}{\max\{1, \log \rho\}}\right)$$

since $\rho = o(n)$ and $\rho \geq 1$.

□

6 Expanding Disk Broadcasting

For the SNR model a simple flooding algorithm works as well as the algorithm we propose. A straight-forward observation is that every increase in sending amplitude and every additional sending node increases the coverage area. For the upper bound we use Algorithm 1 which is slower, yet still asymptotically tight to the lower bound and easier to analyze. We choose $r_{j+1} = \frac{1}{4}\sqrt{\rho}r_j$, starting with $r_1 = 1$ and prove the following Lemma.

Lemma 5. *With high probability in round $j + 1 \geq 2$ all nodes in distance r_{j+1} from the origin have been informed.*

Proof. The expected number of nodes in the disk of radius r_j is $\rho\pi r_j^2$. The maximum distance from any node in the disk of radius r_{j+1} to a node in this disk is at most $r_j + r_{j+1} \leq 2r_{j+1}$. Hence, the received signal has an expected SNR of at least $\frac{\rho\pi r_j^2}{(2r_{j+1})^2} \geq 4$. Using Chernoff bounds the result follows. \square

Algorithm Expanding Disk Broadcast

```

Sender  $v_0$  starts sending
 $j \leftarrow 1$ 
while  $r_j < R$  do
  for all  $v \in \{v_1, \dots, v_n\}$  which are informed and where  $\|v - v_0\|_2 \leq r_j$  do
    Node  $v$  starts sending
  end
   $j \leftarrow j + 1$ 
end
end

```

Algorithm 1: Expanding Disk Broadcast

Therefore $r_j = (\rho/16)^{(j-1)/2}$ and for $j \geq 1 + 2\frac{\log n - \log(\pi\rho)}{(\log \rho) - 4} = \Theta(\log n / \log \rho)$ we have $r_j \geq R$ and all nodes are informed.

Corollary 1. *In the SNR-model collaborative broadcasting needs $\mathcal{O}(\log n / \log \rho)$ rounds for $\rho > 16$, if broadcasting starts with at least $\Omega(\log n)$ nodes, or $\rho = \Omega(\log n)$.*

We conjecture that the result of Corollary 1 not only holds for our (line-of-sight, path loss exponent 2) SNR model but also holds for the model proposed in [31, 15] where the path loss exponent is $\alpha \leq 2$. Then, the channel from sender v_j to receiver v_k has effect $s_j(t) \cdot h_{j,k}(t)$ for emitted signal $s_j(t)$ and $h_{j,k}(t) = \|v_k - v_j\|_2^{-\alpha/2} \cdot e^{i\cdot\theta_{j,k}(t)}$ with random phase shift $\theta_{j,k}(t)$ at time t . We will discuss some further conjectures about the path loss factor in the outlook.

The transmission range grows in each round exponentially with factor $r_j/r_{j-1} = \sqrt{\rho/16}$. In order to minimize this term, we define the radii downwards. Let $p = \lceil 2 \log R / (\log \rho / 16) \rceil$ denote the last round and define $r'_p := R = \sqrt{\frac{n}{\rho\pi}}$.

Then, define $r'_{j-1} := r'_j / \sqrt{\rho/16}$. Note that $r'_j \leq r_1 = 1$ and therefore $r'_2 \leq r_2$ can be informed in one step.

So, the overall time T is mostly determined by the speed of light:

$$T \leq \sum_{j=1}^p r'_j \leq R \left(1 + \sum_{j=1}^{p-1} \frac{1}{(\log \rho / 16)^{j/2}} \right) = R \left(1 + \mathcal{O} \left(\frac{1}{\sqrt{\log \rho}} \right) \right).$$

Since we assume that $\rho = \Omega(\log n)$ we have in this setting the following corollary.

Corollary 2. *The speed of the SNR Broadcast approaches the speed of light for growing n .*

However, the time effort for decoding and encoding at a node is for practical applications usually much larger than the time caused by the speed of light, the main factor is the number of times the signals have to be relayed, i.e. the number of rounds.

7 MISO

In MISO we only analyze the expanding broadcasting algorithm, since the coverage area is far from convex nor does every additional sending node help, see Fig. 4. We use $r_1 = 1$ and the expansion $r_{j+1} = c_1 \rho r_j^{3/2} \lambda^{1/2}$ for a constant c_1 to be defined later. The senders v_k are synchronized with a phase shift $\varphi_\ell = -2\pi\|v_\ell - v_0\|_2/\lambda$ such that the resulting signal of v_ℓ is $e^{i(2\pi t/\lambda + \varphi_\ell)}$.

Theorem 2. *If $r_j \geq \frac{2c_5}{c_2\pi} \frac{\ln n}{\rho}$ then every receiver in distance d can be triggered with high probability, where $15r_j \leq d \leq c_1 r_j^{3/2} \lambda^{1/2}$, for $c_1 = \frac{1}{4}c_3$ and some constants c_3, c_2 , and c_5 defined later.*

Algorithm MISO Broadcast

```

Run Expanding Disk Broadcast for  $R = \frac{2c_5 \ln n}{c_2 \pi \rho}$ 
   $j \leftarrow t$ 
  while  $r_j < R$  do
    for all  $v \in \{v_1, \dots, v_n\}$  which are informed and where  $\|v - v_0\|_2 \leq r_j$  do
      Node  $v$  starts sending with phase shift  $\varphi = -2\pi\|v - v_0\|_2/\lambda$ 
    end
     $j \leftarrow j + 1$ 
  end
end

```

Algorithm 2: MISO Broadcast

Proof. We consider an arbitrary node q in distance d from the first sender v_0 in the center. We prove that this node is triggered with high probability and thus all receivers in this distance will be triggered likewise with this probability.

First we analyze the expected received signal of a receiver in distance d , which is given by an integral. The complex value of this integral will be asymptotically estimated using a geometric argument over the intersection of ellipses with equal phase shift impact and the sender disk.

In this section $m + 1$ denotes the number of triggered senders in a disk of radius r . Sender v_0 resides at $(0, 0)$. The other m senders are uniformly distributed in the disk of radius r . We investigate the received signal rx at a receiver q outside of this disk with distance $d \geq r$. Wlog. we assume q lies on the x -axis.

Define for $p = (p_x, p_y)$:

$$\Delta_d(p) := \sqrt{p_x^2 + p_y^2} + \sqrt{(d - p_x)^2 + p_y^2} - d. \quad (7)$$

Using this notion the received signal strength is given by

Lemma 6. For $0 \leq w \leq \tau + \lambda/2$ and senders $v_1, \dots, v_n \in D(v_0, r)$ the received signal is given as $rx(t) = rx \cdot e^{i2\pi(t-d)/\lambda}$, where $rx = \sum_{j=1}^n \frac{e^{-i2\pi\Delta_d(v_j)/\lambda}}{\|q - v_j\|_2}$.

We will estimate the absolute value $|rx|$ as follows.

First, we see that there is an easy characterization by ellipses E_τ with focal points in v_0 and q , which characterize whether senders help or interfere, see Fig. 5. The parameter τ describes the phase at which the sender's signal arrives at the receiver q . The main contributor to the received signal comes from the area within E_τ which has an area of $\Theta(r^{3/2}\lambda^{1/2})$, which corresponds to the innermost dark ellipse in Fig. 5. The other areas more or less cancel themselves out.

To prove this, we give a formula which describes exactly the expected signal at a given point t_0 . This expectation will be estimated by carefully chosen bounds. We denote by D_r the disk with center $(0, 0)$ and radius r .

Consider the ellipse E_τ with focal points $v_0 = (0, 0)$ and $q = (d, 0)$:

$$E_\tau := \{p \in \mathbb{R}^2 \mid \|p\|_2 + \|p - q\|_2 = d + \tau\}.$$

We will use the following notation to describe all points inside this ellipse:

$$E_{\leq \tau} := \{p \in \mathbb{R}^2 \mid \|p\|_2 + \|p - q\|_2 \leq d + \tau\}.$$

Lemma 7. $\mathbb{E}[rx] = \frac{1}{d} + \frac{m}{2\pi r^2} \iint_{(x,y) \in D_r} \frac{e^{-i\Delta_d(x,y)2\pi/\lambda} dx dy}{\sqrt{(x-d)^2 + y^2}}$.

In order to estimate this expectation we introduce the following terms for the disk $D_r = \{p \in \mathbb{R}^2 \mid \|p\|_2 \leq r\}$.

$$h(w, \lambda, d) := \iint_{(x,y) \in E_{\leq w} \cap D_r} \frac{e^{-i\Delta_d(x,y)2\pi/\lambda}}{\sqrt{(x-d)^2 + y^2}} dx dy. \quad (8)$$

Note that the following relationship holds.

$$\mathbb{E}[rx] = \frac{1}{d} + \frac{m}{2\pi r} h(1, \lambda/r, d/r).$$

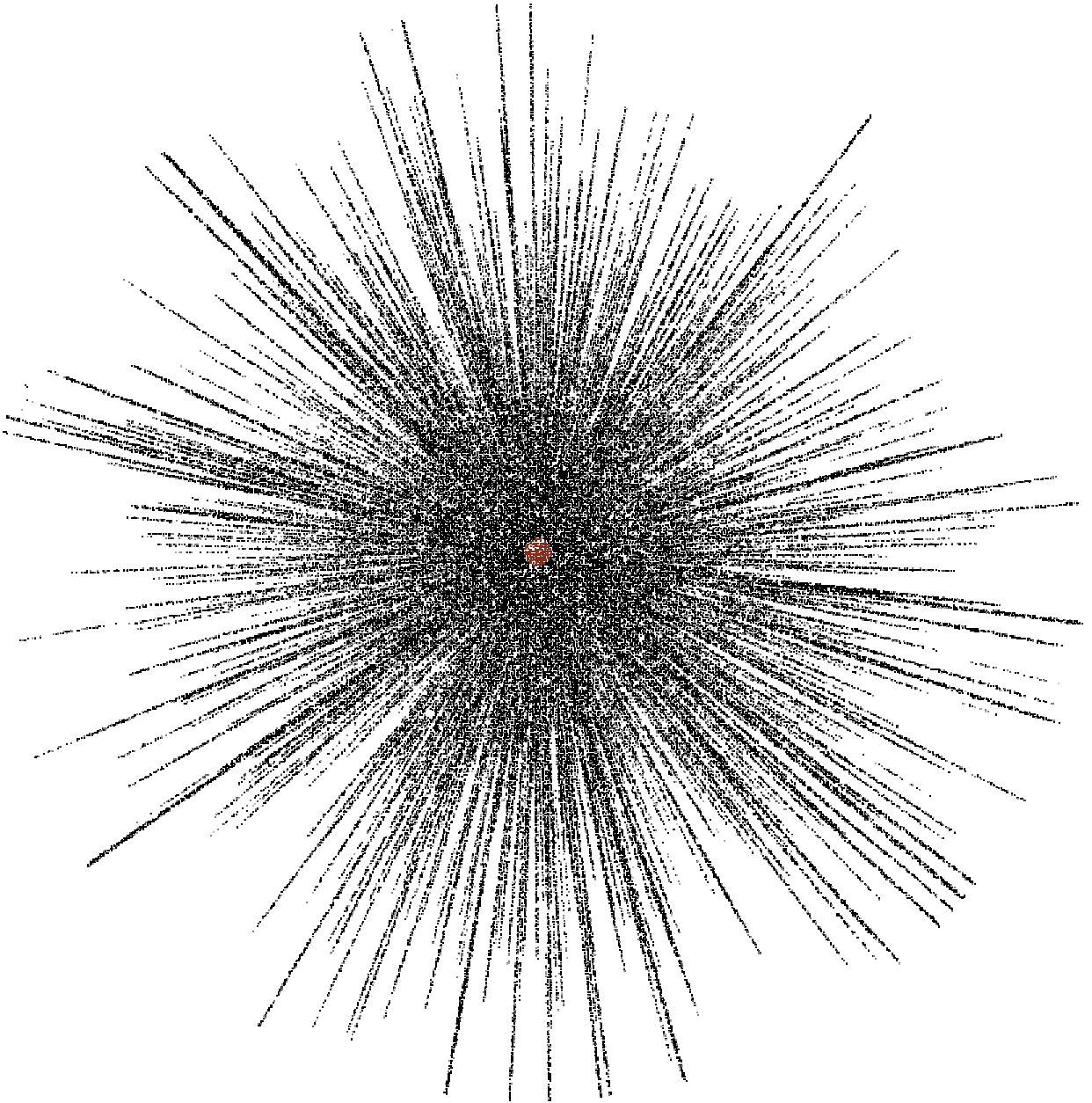


Figure 4: Randomly placed nodes reached by a cooperative broadcast in the MISO model from the set of senders randomly placed in the red disk.

Now the estimation of the signal is based on the following lemma proved in the Appendix, which implies the subsequent Lemma.

Lemma 8. For $\lambda \leq 2$ and $d > 15$:

$$\mathfrak{S}(h(1, d, \lambda)) \geq \frac{9}{2,240\sqrt{2}} \frac{\sqrt{\lambda}}{d+1}. \quad (9)$$

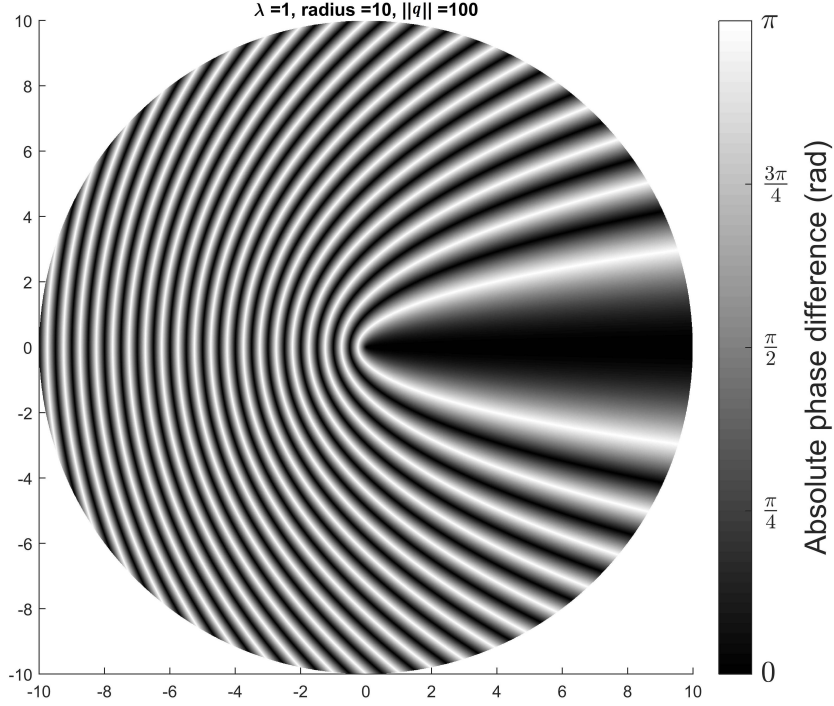


Figure 5: Senders in a disk of radius 10, colored according to the phase difference perceived by a receiver located at point (100, 0) for wavelength 1 [32].

Proof. We need the following definitions, where $h_\infty(w, \lambda)$ is used to estimate the signal energy in the far-distance case. We first estimate its size and then apply it to $h(w, d, \lambda)$.

$$h_\infty(d, \lambda) := \iint_{(x,y) \in E_{\leq w} \cap U} e^{i\Delta_d(x,y)2\pi/\lambda} dx dy \quad (10)$$

$$h(1, d, \lambda) := \iint_{(x,y) \in E_{\leq w} \cap U} \frac{e^{i\Delta_d(x,y)2\pi/\lambda}}{\sqrt{(x-d)^2 + y^2}} dx dy, \quad (11)$$

where $\Delta_d(x, y) := \sqrt{x^2 + y^2} + \sqrt{(d-x)^2 + y^2} - d$.

We use a geometric argument and concentrate on the area of the intersection of the disk U and the $E_{\leq w}$ described by $f(w, d) = \iint_{(x,y) \in E_{\leq w} \cap U} 1 dx dy$. Using the following function for the area of the segment of depth z of an ellipse with radii r_1 and r_2 we derive a closed form for this function, see Fig. 6.

$$g(x) := \arccos(1-x) - (1-x)\sqrt{1-(1-x)^2}$$

$$s(r_1, r_2, z) = r_1 r_2 g\left(\frac{z}{r_1}\right)$$

The main notations are shown in Fig 7. The cutting depth z_0 of the circle and the cutting depth z_1 for the ellipse are

$$z_0 = w \cdot \frac{2d-2+w}{2d}$$

$$z_1 = 1 - z_0 + w/2 = \frac{(2-w)(d+w)}{2d}.$$

Define the derivatives f' and f'' with respect to the first parameter:

$$f'(x, y) := \frac{df(x, y)}{dx} \quad (12)$$

$$f''(x, y) := \frac{d^2 f(x, y)}{dx^2} \quad (13)$$

The following observations of the derivatives are useful later on.

Lemma 9. For $x \in [0, 2]$, $y \geq 1$:

$$f'(x, y) > 0 \quad (14)$$

$$\sqrt{x} < f(x, y) < \frac{7}{3}\sqrt{x} \quad (15)$$

$$\text{For } y \geq 2: \frac{3}{2}\sqrt{x} < f(x, y) \quad (16)$$

$$\text{For } y > 1, x \leq 2: \frac{f(x, y)}{f(x/2, y)} > \frac{7}{5} \quad (17)$$

Proof. Inequality (14) follows by the definition of $f(x, y)$. The other inequalities have been verified by computer generated function tables using interval arithmetics, see also the plots in Figs. 8-15 to get an intuition.

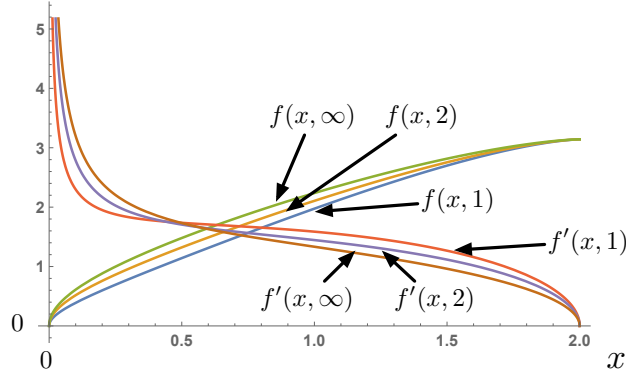


Figure 8: Plot of functions $f(x, y)$ and $f'(x, y)$ for exemplary values $y \in \{1, 2, \infty\}$

In the automated proofs we only use rational numbers and only test if for two numbers $a < b$. The automated proofs check whether for some function h the inequality $h(x) < c$ holds for $x \in [a, b]$, where $h(x)$ is finite in $[a, b]$. For this we divide the interval $[a, b]$ in smaller intervals $[a_0, a_1], [a_1, a_2], \dots, [a_{n-1}, b]$. Then, for an interval we calculate $f([a_j, a_{j+1}]) = [s_j, \ell_j]$ using interval arithmetics [33]. So, it holds that $s_j \leq f(x) \leq \ell_{j+1}$ for all $x \in [a_j, a_{j+1}]$. Then, we check whether $\ell_j < c$ for all i . If this is not the case, we increase the number of intervals n to have smaller intervals. By basic analysis it follows that a set of small enough intervals must exist that deliver a positive result if $h(x) < c$.

Analogously, we generate proofs for two-dimensional cases to check that $f(x, y) < c$ holds for $x \in [a, b], y \in [a', b']$, where we use input intervals $[a_j, a_{j+1}] \times [a'_k, a'_{k+1}]$.

However, a direct application is not possible before we have not resolved the following two problems: we have an open interval $y \in [1, \infty)$ and some comparisons involve functions on both side of the inequality.

For the first problem we substitute $z = \frac{1}{y}$ and consider functions over the interval $z \in [0, 1]$. At $z = 0$ we have to show that the discontinuity is removable. This way we prove inequality (17) noting that $\lim_{y \rightarrow \infty} \frac{f(2, y)}{f(1, y)} = \sqrt{2} \geq \frac{7}{5}$.

For the second problem we divide by one side and get a removable discontinuity. In order to remove the discontinuity at $x = 0$ for $f(x, y)/\sqrt{x}$, we observe that

$$\lim_{y \rightarrow \infty} f(x, y) = \frac{1}{3}(x+1)\sqrt{(2-x)x} + \arccos(1-x)$$

such that we get a removable discontinuity for $\frac{f(x, y)}{\sqrt{x}}$ for $y \rightarrow \infty$. Using the substitution $z = 1/y$ the automatic selection of intervals for interval arithmetics produces the proofs for inequalities (15) and (16). \square

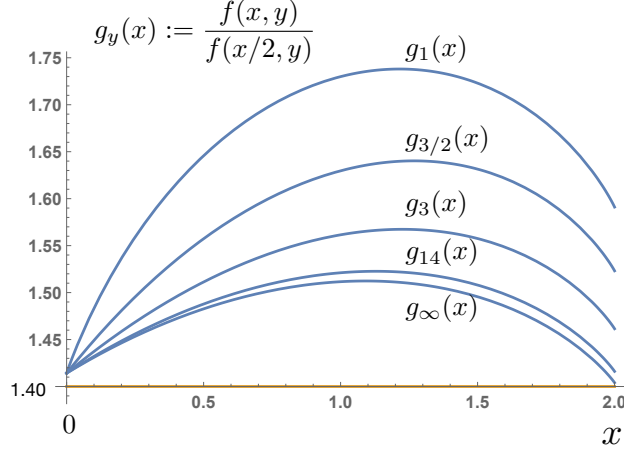


Figure 9: The function $f(x, y)/f(x/2, y)$ for $y \in \{1, 3/2, 3, 14, \infty\}$ relevant for inequality (17)

For (12), (15), (16) f, g , the first and second derivatives of f are the following.

$$\begin{aligned}
 f(x, y) &= g\left(\frac{x(x+2y-2)}{2y}\right) \\
 &\quad + \frac{1}{4}(x+y)\sqrt{x(x+2y)}g\left(\frac{2-x}{y}\right) \\
 \frac{d g(x)}{d x} &= \sqrt{1-(1-x)^2} \\
 f'(x, y) &:= \frac{d f(x, y)}{d y} \\
 &= g\left(\frac{2-x}{y}\right) \frac{2x^2+4xy+y^2}{4\sqrt{x(x+2y)}} \\
 &\quad + \frac{(x+y-2)\sqrt{x(2-x)(x+2y-2)(x+2y)}}{2y^2} \\
 f''(x, y) &:= \frac{d^2 f(x, y)}{d^2 y} = T_1(x, y) + T_2(x, y) + T_3(x, y),
 \end{aligned}$$

where we have the following terms.

$$\begin{aligned}
 T_1(x, y) &= \frac{-3x^4 - 2x^3(6y-7) - 2x^2(7y^2-21y+10) - 4x(y^3-8y^2+10y-2) + 4y(y^2-3y+2)}{2y^2\sqrt{(2-x)x(x+2y-2)(x+2y)}} \\
 T_2(x, y) &= -\frac{\sqrt{(2-x)(x+2y-2)}(2x^2+4xy+y^2)}{2y^2\sqrt{x(x+2y)}} \\
 T_3(x, y) &= \frac{(x+y)(2x^2+4xy-y^2)}{4(x(x+2y))^{3/2}}g\left(\frac{2-x}{y}\right)
 \end{aligned}$$

We can prove via interval arithmetics for $x \in [0, 2], y \geq 1$ the following inequalities, see also Figures 10, 11, 12, 13.

Lemma 10. *The following inequalities hold for $y \geq 1, x \in [0, 2]$:*

$$-2 \leq T_1(x, y)\sqrt{x(2-x)} \leq 2 \quad (18)$$

$$-3 \leq T_2(x, y)\sqrt{x} \leq 0 \quad (19)$$

$$-1 \leq T_3(x, y)x^{3/2} \leq 1 \quad (20)$$

$$1 \leq \frac{g(x)}{x^{3/2}} \leq 2. \quad (21)$$

For $x \in (0, \frac{1}{100}]$, $y \geq 1$

$$T_3(x, y)x^{3/2} \leq -\frac{1}{5}. \quad (22)$$

where discontinuities at $x = 0$ and $x = 2$ are removed.

For $x \in [\frac{1}{100}, 2 - \frac{1}{100}]$, $y \geq 1$

$$f''(x, y) \leq -\frac{1}{8}. \quad (23)$$

Proof. Possible discontinuities at $x = 0$ and $x = 2$ of the functions $T_1(x, y)\sqrt{x(2-x)}$, $T_2(x, y)\sqrt{x}$, and $T_3(x, y)x^{3/2}$ can trivially be removed by algebraic transformation. The function $\frac{g(x)}{x^{3/2}}$ is also finite with a removable discontinuity at $x = 0$, since

$$\lim_{x \rightarrow 0} \frac{g(x)}{x^{3/2}} = \frac{4}{3}\sqrt{2},$$

which can be seen by the Taylor series. For the automated proofs we again replace $z = \frac{1}{y}$ and prove the claims for the interval $z \in [0, 1]$ with interval arithmetics.

Since f'' is finite over this domain, we can apply an automated proof with interval arithmetics for $f''(x, 1/z) < -\frac{1}{8}$ for $x \in [1/100, 1 - 1/100]$, removing the discontinuity for $z = 0$. \square

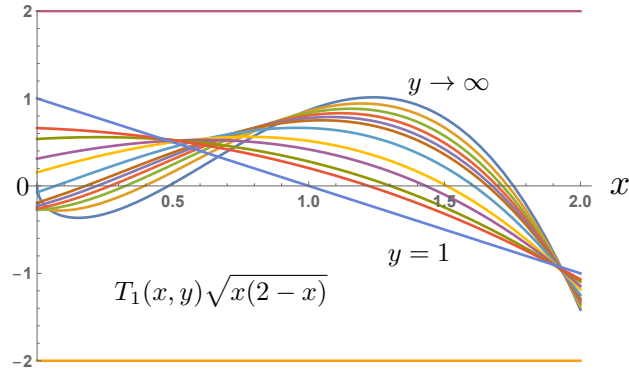


Figure 10: The function $T_1(x, y)\sqrt{x(2-x)}$ for $y \in \{1, 1.1, 1.2, 1.3, 1.4, 1.5, 1.8, 2.5, 3.2, 5, 7, \infty\}$, relevant for Inequality (18)

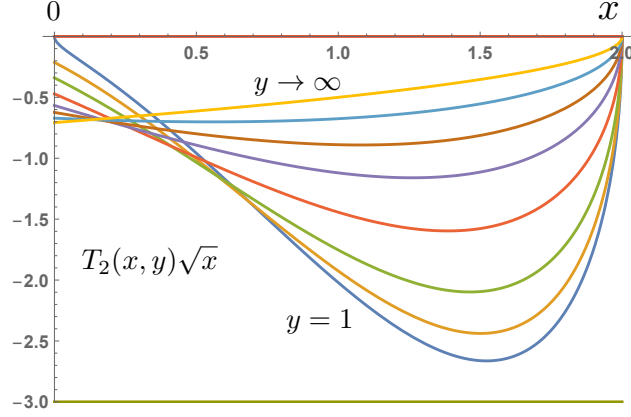
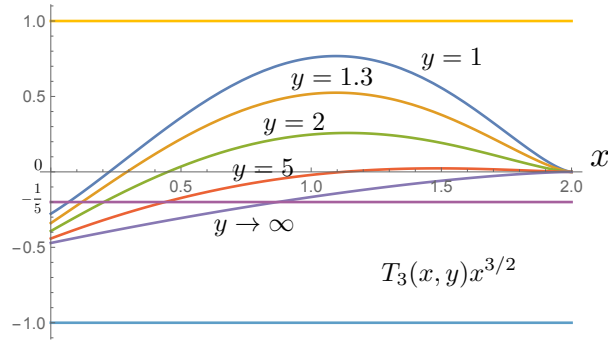
Lemma 11. For all $y > 1$, $x \in (0, 2)$

$$f''(x, y) < -\frac{1}{4}.$$

For $x \in [2 - \frac{1}{100}, 2)$, $y \geq 1$

$$f''(x, y) \leq -199. \quad (24)$$

Proof. The second derivative $f''(x)$ tends to $-\infty$ at the borders of $x \in [0, 2]$. We have proved (22) via interval arithmetics for $x \leq \frac{1}{100}$: $x^{3/2}T_3(x, y) \leq -1/5$. Then, it follows for $x \in [0, \frac{1}{100}]$:

Figure 11: The function $T_2(x, y)\sqrt{x}$ for $y \in \{1, 1.1, 1.3, 1.8, 2.8, 4.5, 10, \infty\}$, relevant for inequality (19)Figure 12: The function $T_3(x, y)x^{3/2}$ for $y \in \{1, 1.3, 2, 5, \infty\}$, relevant for inequality (20)

$$\begin{aligned}
 f''(x, y) &\leq T_3(x, y) + \frac{2}{\sqrt{x(2-x)}} \\
 &\leq -\frac{1}{5x^{3/2}} + \frac{2\sqrt{x}}{\sqrt{(2-x)}} \\
 &= \frac{1}{\sqrt{x}} \left(-\frac{1}{5x} + \frac{2x}{\sqrt{(2-x)}} \right) \\
 &< -199
 \end{aligned}$$

For $x \geq 2 - \frac{1}{100}$ we get

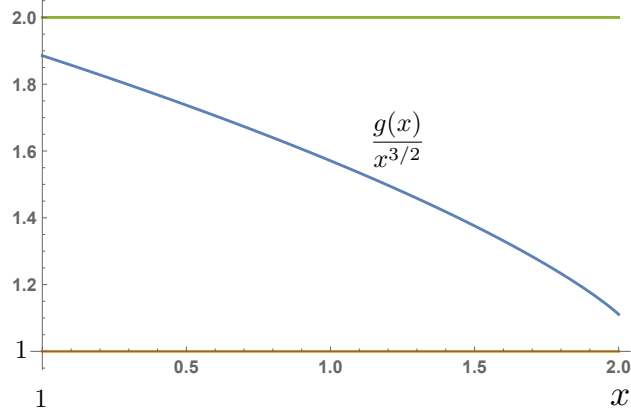
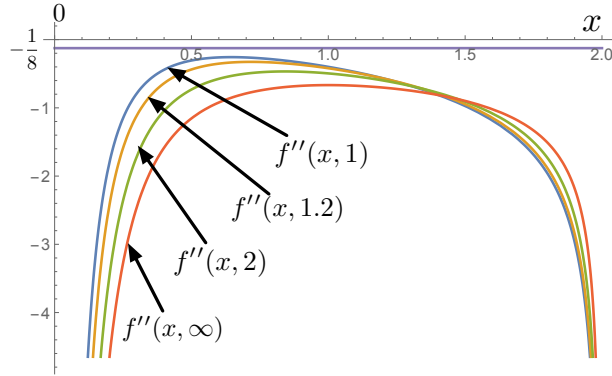
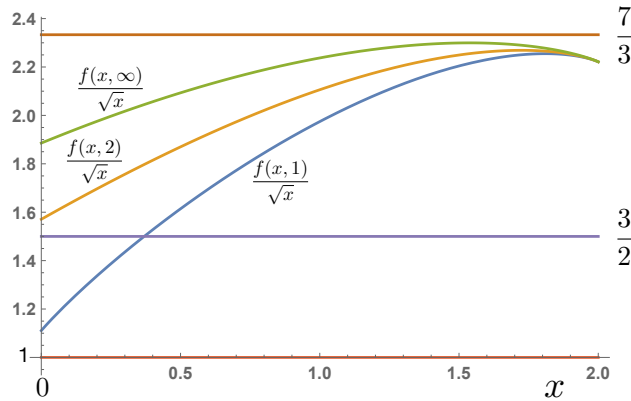
$$\begin{aligned}
 f''(x, y) &\leq T_1(x, y) + T_2(x, y) + T_3(x, y) \\
 &\leq -\frac{1}{2}\sqrt{x(2-x)} + x^{3/2} \\
 &\leq -\frac{\sqrt{100}}{2\sqrt{2 - \frac{1}{100}}} + (2 - 1/100)^{3/2} \\
 &< -7/5
 \end{aligned}$$

□

These lemmas imply:

Lemma 12. For $x \in (0, 2), y \geq 1$:

$$f''(x, y) \leq -\frac{1}{8}.$$

Figure 13: The function $g(x)/x^{3/2}$, relevant for inequality (21)Figure 14: The function $f''(x, y)$ for $y \in \{1, 1.2, 2, \infty\}$ of Lemma 11Figure 15: The function $f(x, y)/\sqrt{x}$ for $y \in \{1, 2, \infty\}$ relevant for inequalities (15) and (16)

Using f we can describe h_∞ as follows.

Lemma 13. For $w \in [0, 2]$:

$$h_\infty(w, d) = \int_{x=0}^w e^{i2\pi x/\lambda} f'(x, d) dx .$$

Proof. Be the above considerations we know that the area of $E_{\leq w} \cap U$ is described by $f(w, d)$. Hence, the differential area with points with phase w is given by

$$\frac{d f(w, d)}{d w} = f'(w, d).$$

□

For the orientation of $h_\infty(w, d)$ we get the following Lemma.

Lemma 14. For all $w \geq 0$:

$$\arg(h_\infty(w, d)) \in (0, \pi)$$

Proof. We extend $f'(x, y)$ as $f'(x, y) = 0$ for $y \geq 2$. We consider two consecutive intervals of distance λ :

$$\begin{aligned} h_\infty(w) &= \sum_{j=0}^{\lceil 2/\lambda \rceil} \int_{x=0}^{\lambda} e^{i2\pi x/\lambda} f'(x + j\lambda, d) dx \\ &= \sum_{j=0}^{\lceil 2/\lambda \rceil} \int_{x=0}^{\lambda/2} e^{i2\pi x/\lambda} \left(f'(x + j\lambda, d) f' \left(x + j\lambda + \frac{1}{2}\lambda, d \right) \right) dx \\ &= \int_{x=0}^{\lambda/2} e^{i2\pi x/\lambda} \sum_{j=0}^{\lceil 2/\lambda \rceil} \left(f'(x + j\lambda, d) - f' \left(x + j\lambda + \frac{1}{2}\lambda, d \right) \right) dx \end{aligned}$$

Since $f''(x, y) \leq -\frac{1}{8}$ we have

$$f'(x + j\lambda, d) - f' \left(x + j\lambda + \frac{1}{2}\lambda, d \right) \geq \frac{1}{16}\lambda$$

Because every difference is positive and it follows that $\arg_\infty(w) \in (0, \pi)$. □

From this consideration one can only imply that $\Im(h_\infty(w)) = \Omega(\lambda)$. To achieve a better bound we concentrate on the term of the sum.

Proposition 1. For $x \leq \lambda/2$:

$$f'(x, d) \geq \frac{7}{5} f' \left(x + \frac{1}{2}\lambda, d \right)$$

Proof. Since $x \leq \lambda/2$ we have $2x \leq x + \lambda$ and by Lemma 9 and the monotony of f' it follows:

$$f'(x, d) \geq \frac{7}{5} f'(2x, d) \geq \frac{7}{5} f' \left(x + \frac{1}{2}\lambda, d \right).$$

□

Proposition 2.

$$\Im(h_\infty(w)) \geq \int_{x=0}^{\lambda} \sin(2\pi i x/\lambda) f'(x, d) dx.$$

Proof. Because $f''(x, y) < 0$ the other sum terms for $j > 0$ may only increase the imaginary terms. □

Proposition 3.

$$\int_{x=0}^{\lambda/2} \sin(2\pi i x/\lambda) f'(x, d) dx \geq \frac{2}{7} \int_{x=0}^{\lambda} \sin(2\pi i x/\lambda) f'(x, d) dx$$

Proof. For $x \leq \lambda$ by the claim above we have:

$$f'(x, d) \geq \frac{7}{5} f'(x + \lambda/2, d)$$

Hence

$$f'(x, d) - f'(x + \lambda/2, d) \geq \frac{2}{7} f'(x, d).$$

□

Proposition 4. For $d \geq 2$

$$\int_{x=0}^{\lambda/2} \sin(2\pi i x/\lambda) f'(x, d) dx \geq \frac{1}{16\sqrt{2}} \sqrt{\lambda}$$

Proof. We use that $\frac{3}{2}\sqrt{x} < f(x, y) < \frac{7}{3}\sqrt{x}$ from (25) and that $f'(x, y)$ decreases with x (Lemma 12).

$$\begin{aligned} \int_{x=0}^{\lambda/2} \sin(2\pi i x/\lambda) f'(x, d) dx &\geq \int_{x=\lambda/4}^{\frac{3}{4}\lambda} \sin(2\pi i x/\lambda) f'(x, d) dx \\ &\geq \int_{x=\lambda/4}^{\frac{3}{4}\lambda} \frac{1}{\sqrt{2}} f'(x, d) dx \\ &\geq \int_{x=\lambda/4}^{\frac{3}{4}\lambda} \frac{1}{\sqrt{2}} f'(x, d) dx \\ &\geq \frac{1}{2\sqrt{2}} \left(f\left(\frac{3}{4}\lambda, d\right) - f\left(\frac{1}{4}\lambda, d\right) \right) \\ &\geq \frac{1}{2\sqrt{2}} \left(\frac{3}{2}\sqrt{\frac{3}{4}\lambda} - \frac{7}{3}\sqrt{\frac{1}{4}\lambda} \right) \\ &\geq \frac{\frac{3}{2}\sqrt{3} - \frac{7}{3}}{4\sqrt{2}} \lambda^{1/2} \\ &\geq \frac{1}{16\sqrt{2}} \lambda^{1/2} \end{aligned}$$

□

This implies the following Lemma:

Lemma 15. For $w \geq \lambda/2$, $d \geq 2r$:

$$\Im(h_\infty(w, \lambda)) \geq \frac{1}{56\sqrt{2}} \sqrt{\lambda}.$$

Proof. Follows by the combining the above claims.

□

We now estimate for $d \geq c_f \lambda + 1$:

$$h(w, \lambda) := \iint_{(x,y) \in E_{\leq w} \cap U} \frac{e^{2\pi i \Delta_d(x,y)/\lambda}}{\sqrt{(x-d)^2 + y^2}} dx dy.$$

where $\Delta_d(p) := \|p\|_2 + \|p - q\|_2 - d$. We change coordinates from (x, y) to (z, ℓ) , where z is the x -coordinate of the Ellipse E_w and ℓ is the distance from the point to the receiver. Note that

$$\begin{pmatrix} x(\ell, z) \\ y(\ell, z) \end{pmatrix} = \begin{pmatrix} \frac{2d^2 - 2d\ell + 2dz - 2\ell z + z^2}{2d} \\ \frac{\sqrt{z}\sqrt{2\ell - z}\sqrt{4d^2 - 4d\ell + 4dz - 2\ell z + z^2}}{2d} \end{pmatrix}$$

Lemma 16. For $0 \leq w \leq 2$:

$$h(w, \lambda) = \int_{z=0}^w \int_{\ell=d-1+z}^{d+z/2} 2 \frac{e^{2\pi iz/\lambda}}{\ell} |\det(\phi(\ell, z))| d\ell dz$$

where for $\ell \geq z$:

$$|\det(\phi(\ell, z))| = \frac{2\ell(d-\ell+z)}{\sqrt{z}\sqrt{2\ell-z}\sqrt{(2d+z)(2d-2\ell+z)}}$$

where $\phi(\ell, z)$ is the Jacobian of $\begin{pmatrix} x(\ell, z) \\ y(\ell, z) \end{pmatrix}$.

Proposition 5.

$$f'(z, d) = \int_{\ell=d-1+z}^{d+z/2} 2 |\det(\phi(\ell, z))| d\ell$$

Define

$$t(d, z, \ell) := \int_{\ell=d-1+z}^{d+z/2} \frac{2}{\ell} |\det(\phi(\ell, z))| d\ell.$$

Lemma 17. For $d > 1$ and $\ell \in [d-1, d+1]$ for all $w \in [0, 2]$:

$$\frac{f'(z, d)}{d+1} \leq t(d, z, \ell) \leq \frac{f'(z, d)}{d+1} \left(1 + \frac{2}{d-1}\right)$$

Proof. Note that $0 < d-1 \leq \ell \leq d+1$. Hence,

$$\frac{1}{d+1} \leq \frac{1}{\ell} \leq \frac{1}{d-1} = \frac{1}{d+1} \left(1 + \frac{2}{d-1}\right)$$

□

We choose $d \geq 15$ and get $\frac{2}{d-1} \leq \frac{1}{7}$.

Lemma 18. For $w \geq \lambda/2$, $d \geq 15$:

$$\Im(h(w)) \geq \frac{1}{112\sqrt{2}(d+1)} \sqrt{\lambda}.$$

Proof. We consider two consecutive intervals of distance λ :

$$\begin{aligned} h(w, d) &= \sum_{j=0}^{\lceil 2/\lambda \rceil} \int_{z=0}^{\lambda} \int_{\ell=d-1+z+j\lambda}^{d+(z+j\lambda)/2} 2 \frac{e^{2\pi iz/\lambda}}{\ell} |\det(\phi(\ell, z))| d\ell dz \\ &= \sum_{j=0}^{\lceil 2/\lambda \rceil} \int_{z=0}^{\lambda/2} \frac{e^{2\pi iz/\lambda}}{\ell} (t(d, z+j\lambda, \ell) - t(d, z+j\lambda+\lambda/2, \ell)) dz \end{aligned}$$

Now for $z \leq \lambda/2$, $d \geq 15$:

$$t(d, z+\lambda/2, \ell(x, y)) \leq \frac{8}{7} \frac{1}{d+1} f'(z+\lambda/2, d) \tag{25}$$

$$\leq \frac{8}{7} \cdot \frac{5}{7} \cdot \frac{1}{d+1} f'(z/2 + \lambda/4, d)$$

$$\leq \frac{8}{7} \cdot \frac{5}{7} \cdot \frac{1}{d+1} f'(z, d) \tag{26}$$

$$\leq \frac{40}{49} t(d, z, \ell(x, y))$$

The first line (25) follows from Lemma 17. Line (26) follows from $z/2 + \lambda/4 \geq z$ and that f' is monotone decreasing because $f''(x, y) < -\frac{1}{8}$ by Lemma 12.

Hence $t(d, z, \ell(x, y)) - t(d, z + \lambda/2, \ell(x, y)) \geq \frac{9}{40}t(d, z, \ell(x, y))$ which we use in line 27:

$$\begin{aligned}
\Im(h(w)) &= \sum_{j=0}^{\lceil 2/\lambda \rceil} \int_{z=0}^{\lambda} \frac{\sin(2\pi i z/\lambda)}{\ell} t(d, z + j\lambda, \ell(x, y)) \, d\ell \, dz \\
&\geq \sum_{j=0}^{\lceil 2/\lambda \rceil} \int_{z=0}^{\lambda/2} \frac{9}{40} \frac{\sin(2\pi i z/\lambda)}{\ell} t(d, z + j\lambda, \ell(x, y)) \, d\ell \, dz \\
&\geq \sum_{j=0}^{\lceil 2/\lambda \rceil} \int_{z=0}^{\lambda/2} \frac{9}{40} \frac{\sin(2\pi i z/\lambda)}{d+1} f'(z + j\lambda, d) \, dz \\
&\geq \frac{9}{40} \frac{1}{d+1} \sum_{j=0}^{\lceil 2/\lambda \rceil} \int_{z=0}^{\lambda} \sin(2\pi i z/\lambda) f'(z + j\lambda, d) \, dz \\
&= \frac{9}{40} \frac{1}{d+1} \Im(h_\infty(2, \lambda)) \\
&\geq \frac{1}{56\sqrt{2}} \frac{9}{40} \frac{1}{d+1} \sqrt{\lambda} \\
&\geq \frac{9}{2,240\sqrt{2}} \frac{\sqrt{\lambda}}{d+1}
\end{aligned} \tag{27}$$

$$\begin{aligned}
&= \frac{9}{40} \frac{1}{d+1} \Im(h_\infty(2, \lambda)) \\
&\geq \frac{1}{56\sqrt{2}} \frac{9}{40} \frac{1}{d+1} \sqrt{\lambda} \\
&\geq \frac{9}{2,240\sqrt{2}} \frac{\sqrt{\lambda}}{d+1}
\end{aligned} \tag{28}$$

□

In line (28) we use the definition of h_∞ and then apply Lemma 15.

This completes the proof of Theorem 2. The size of the constant factors have suffered under the many approximations and are far from the truth. Nevertheless the asymptotic behavior matches the lower bound. □

Lemma 19. For $d > 15r$: $\mathbb{E}[\Im[rx]] \geq \frac{9}{4,480\pi\sqrt{2}} \frac{m\sqrt{\lambda}}{d\sqrt{r}}$.

Proof. $\mathbb{E}[\Im[rx]] \geq \frac{m}{2\pi r} \frac{9}{2,240\sqrt{2}} \frac{\sqrt{\lambda/r}}{d/r+1} \geq \frac{9}{4,480\pi\sqrt{2}} \frac{m\sqrt{\lambda}}{d\sqrt{r}}$. □

We apply the Hoeffding bound (Theorem 2 of [34]), which states for n independently distributed random variables $X_j \in \mathbb{R}$ strictly bounded by the intervals $[a_j, b_j]$:

$$\text{Prob} \left[|\bar{X} - \mathbb{E}[\bar{X}]| \geq t \right] \leq 2 \exp \left(- \frac{2n^2 t^2}{\sum_{j=1}^n (b_j - a_j)^2} \right), \text{ where } \bar{X} = \frac{1}{n} \sum_{j=1}^n X_j.$$

We will use $X_j = \Im \left[\frac{e^{2\pi i \Delta_d(v_j)/\lambda}}{\|q - v_j\|_2} \right] \in \left[-\frac{1}{d-r}, \frac{1}{d-r} \right] =: [a_j, b_j]$ denoting the signal produced by each of the m central senders. Furthermore, we set $t = \frac{1}{2} \mathbb{E}[\bar{X}]$. Hence, $a_j - b_j = \frac{2}{d-r} \geq \frac{2}{d-\frac{1}{15}d} \geq \frac{30}{14d}$.

Note that $\mathbb{E}[\bar{X}] \geq c_3 \sqrt{\frac{\lambda}{r}} \frac{1}{d} \geq c_3 \sqrt{\frac{\lambda}{r}} \frac{14}{30} (a - b)$, where $c_3 = \frac{9}{4,480\pi\sqrt{2}}$. Therefore

$$\frac{t^2}{(b-a)^2} = \frac{\frac{1}{4} \mathbb{E}[\bar{X}]^2}{(b-a)^2} \geq c_3^2 \left(\frac{14}{30} \right)^2 \frac{\lambda}{r}$$

This implies the following Lemma.

Lemma 20. For $d \geq 15r$ and $c_4 = \frac{1}{2}c$ and $c_2 = 2c_3^2 \left(\frac{14}{30} \right)^2$

$$\text{Prob} \left[\Im[rx] \leq c_4 \frac{m\sqrt{\lambda}}{d\sqrt{r}} \right] \leq 2 \exp \left(-c_2 \frac{\lambda m}{r} \right).$$

Now $\mathbb{E}[m] = \rho\pi r^2 \geq 2\frac{c_5}{c_2}\frac{r}{\lambda}\ln n$ for $r \geq \frac{2c_5\ln n}{c_2\pi\rho} = \mathcal{O}(\log n/\log \rho)$. Using a Chernoff bound one sees that $m \geq \frac{c_5}{c_2}\frac{r}{\lambda}\ln n$ holds with high probability yielding a probability of $2n^{-c_5}$, where c_5 can be chosen as a constant. Note that $\Im(z) \geq a$ implies $|z|^2 = \Im(z)^2 + \Re(z)^2 \geq a^2$.

Lemma 21. For $r \geq \frac{2c_5}{c_2\pi}\frac{\ln n}{\rho}$ and $d > 15r$: $\text{Prob}\left[|rx|^2 \geq \left(c_4\frac{m\sqrt{\lambda}}{d\sqrt{r}}\right)^2\right] \leq 2n^{-c_5}$.

The right side is larger than the SNR threshold $\beta = 1$ if

$$d \leq \frac{1}{2}c_4\rho\pi r^{3/2}\lambda^{1/2} = \frac{1}{4}c r^{3/2}\lambda^{1/2}$$

Using that $m \geq \frac{1}{2}\rho\pi r^2$ this implies the main Theorem. \square

Theorem 3. MISO broadcasting takes $\mathcal{O}(\log \log n - \log \log \rho + (\log \frac{1}{\lambda})/\log \rho)$ rounds to broadcast the signal.

Proof. The algorithm works in two phases. In the first, we use the SNR variant by choosing random phase shifts. We have seen that then the superposition model breaks down to the SNR model. As shown above we increase $r_{j+1} = \frac{1}{4}\sqrt{\rho}r_j$ until in round t we have $r_j \geq \frac{2k}{c_2\pi}\frac{\ln n}{\rho}$ and $r_j \geq 15r_{j-1}$. This takes at most $t = \mathcal{O}\left(1 + \frac{\log n \log n + \log \frac{1}{\lambda}}{\log \rho}\right)$ rounds.

In the second phase we use the phase shift $\varphi_\ell = \|v_\ell - v_0\|_2$ for all senders v_ℓ . Now the radii increase double exponentially with $r_{j+1} = \frac{1}{4}c\rho r_j^{3/2}\lambda^{1/2}$. After additional $j - t = \mathcal{O}(\log \log n - \log \log \rho)$ rounds we have reached

$$r_j = r_t^{\left(\frac{3}{2}\right)^{j-t}} \left(c_1\rho\lambda^{\frac{1}{2}}\right)^{1+\frac{3}{2}+\dots+\left(\frac{3}{2}\right)^{j-t-1}} = r_t^{\left(\frac{3}{2}\right)^{j-t}} \left(c_1\rho\lambda^{\frac{1}{2}}\right)^{2\left(\frac{3}{2}\right)^{j-t}-2} \geq R = \sqrt{\frac{n}{\pi\rho}}.$$

Note that in round j the nodes in distance r_{j+2} are already triggered. However, the nodes in distance r_{j+1} are too close to the sender area to be safely triggered. This is an implication from Theorem 2. So, it follows that all nodes are then triggered. \square

The tightness of this claim follows from the considerations in [22] and [35] and more extensive in [23] where a lower bound of $\Omega(\log \log n)$ rounds for the unicast problem has been shown. Here, we adapt this argument to include the density ρ .

Lemma 22. Assuming that randomly placed senders are in a disk of radius r , then the maximum distance of a node which can be activated is at most $4\pi\rho r^2$ with high probability for $\rho r^2 = \Omega(\log n)$.

Proof. The expected number of senders in a disk of radius r is $\pi\rho r^2$. Using Chernoff bounds and $\rho r^2 = \Omega(\log n)$ one can show that this number does not exceed $2\pi\rho r^2$ with high probability.

Now, in the best case all waves at a receiver r perfectly add up resulting in a received signal of at most $|rx| \leq \sum_{i=1}^{2\pi\rho r^2} \frac{1}{\|r-s_i\|_2}$. We overestimate this signal by replacing the denominator with $d - r$, where d is the distance of the receiver from the senders' disk's center. Hence, we receive a signal if $|rx|^2 = (2\pi\rho r^2)^2 \geq (d - r)^2$. So, we get $d \leq r + 2\pi\rho r^2 \leq 4\pi\rho r^2$. \square

This Lemma implies the following lower bound.

Corollary 3. Any broadcast algorithm using MISO needs at least $\Omega(\log \log n - \log \log \rho)$ rounds to inform all n nodes with high probability.

Proof. We use Lemma 22 by overestimating the effect of triggered nodes which are bound to disks with radii r_j . We assume that we start with $r_0 = \log n$ for $\rho \geq 1$. Now, let $r_{j+1} = 4\pi\rho r_j^2$ denote the largest distance of a node in the next round.

So $r_j \leq (4\pi\rho \log n)^{2^j}$, which reaches $R - 1 = \sqrt{n/(\pi\rho)} - 1$ at the earliest for some $j = \Omega(\log \log n - \log \log \rho)$. \square

8 Conclusions

We have compared the number of rounds of collaborative broadcasting in three communication models. All of them were derived from the far-field superposition MISO model where the signal-to-noise ratio allows a communication range of one unit.

The first is the Unit-Disk-Graph model. Typically, parallel communication is seen here as a problem, resulting in the Radio Broadcasting model. For the Unit Disk Graph such interference results only in an extra overhead of a constant factor [5]. The delimiting factor is the diameter of the graph, proportional to $\sqrt{n/\rho}$.

For the SNR-model one can achieve broadcasting in a logarithmic number of rounds which comes from the addition of the senders' signal energy. This allows to extend the disk of informed nodes by a factor of $\Theta(\sqrt{\rho})$, where ρ is the sender density. This result is not surprising, since the area grows quadratically in the diameter and the path loss is to the power of two as well, which fits well to the law of conservation of energy.

For the MISO model it is well known that beamforming increases the energy beyond the SNR model. It is possible to achieve logarithmic number of rounds for unicast on the line [22] and $\mathcal{O}(\log \log n)$ for the plane [21]. The used beams are very narrow and for a growing number of sender nodes the ratio between beam range and angle decreases. So, the extended range results from the focus of the energy on a smaller beam, while the signal energy is reduced elsewhere.

This leads to the question, how it is possible that a broadcast with high signal strength can take place. The answer is, that this panoramic beam draws its increased energy from a signal reduction from the three-dimensional space into the two-dimensional space, where the receivers happen to be located.

9 Outlook

We have focused on broadcasting only a single sine signal and not a message consisting of many different signals. There, one faces inter-signal interference and inter-symbol interference. For inter-signal interference, note that the received signal has a constant phase shift. We bounded the interference of non-synchronized signals only by a constant factor with respect to the main signal. So, tighter bounds are necessary. For the inter-symbol interference, a special encoding may reduce the interference caused by signals used for other parts of the message.

In [35] we have described a $\mathcal{O}(\log \log n)$ unicast algorithm without the need of perfect synchronization. There is some hope that a similar technique works here, too. Furthermore, the question remains open whether flooding in MISO is as efficient as the broadcasting algorithm relying on the Expanding Disk Algorithm.

Another interesting question concerns the influence of the path loss exponent α , which we choose as $\alpha = 2$. It has no influence to the UDG model. As an anonymous reviewer pointed out in the SNR model one expects for $\alpha < 2$ a bound of $\mathcal{O}(\log \log n)$ for broadcasting, for $\alpha = 2$ we have proved a bound of $\Theta(\log n)$ and for $\alpha > 2$ a bound of $\mathcal{O}(n^{1/2})$ like in the UDG model is to be expected.

For MISO our results are clearly valid for $\alpha \leq 2$. For larger path loss, we conjecture that the $\mathcal{O}(\log \log n)$ bound for MISO holds for $\alpha < 3$ because of area size of around $\Theta(r^{3/2}\lambda^{1/2})$ of nearly synchronous senders. For larger path loss the asymptotic number of rounds increase. First for $\alpha = 3$ we expect a logarithmic bound and then the same behavior as in the Unit Disk Graph. However, these conjectures need to be proven in future work.

Finally, the communication model is still very simple. Instead of a constant signal-to-noise ratio one might consider Gaussian noise. It is also unclear how obstacles influence the algorithm, or for which other path loss exponents, the double logarithmic number of rounds can be guaranteed.

10 Acknowledgments

We like to thank the organizers of the Dagstuhl Seminar 17271, July 2 - 7, 2017, Foundations of Wireless Networking, where this research was begun and first results have been found. We would also like to thank Alexander Leibold, who performed and checked the automated proofs and anonymous reviewers of a previous version for their detailed and valuable input. We want to thank also Tigrun Tonoyan, Magnus Halldorsson and Zvi Lotker for many fruitful discussions.

References

- [1] David Peleg. Time-efficient broadcasting in radio networks: A review. In *International Conference on Distributed Computing and Internet Technology*, pages 1–18. Springer, 2007.
- [2] Brent N. Clark, Charles J. Colbourn, and David S. Johnson. Unit disk graphs. *Discrete Mathematics*, 86(1–3):165–177, 1990.
- [3] Olga Goussevskaia, Yvonne Anne Oswald, and Rogert Wattenhofer. Complexity in Geometric SINR. In *Proceedings of the 8th ACM international symposium on Mobile ad hoc networking and computing, MobiHoc '07*, pages 100–109, New York, NY, USA, 2007. ACM.
- [4] David Tse and Pramod Viswanath. *Fundamentals of wireless communication*. Cambridge University Press, New York, NY, USA, 2005.
- [5] Rajiv Gandhi, Arunesh Mishra, and Srinivasan Parthasarathy. Minimizing broadcast latency and redundancy in ad hoc networks. *IEEE/ACM Transactions on Networking (TON)*, 16(4):840–851, 2008.
- [6] E. Lebhar and Z. Lotker. Unit disk graph and physical interference model: Putting pieces together. In *IEEE International Symposium on Parallel Distributed Processing (IPDPS 2009)*, pages 1–8, may 2009.
- [7] Magnús M. Halldórsson and Tigran Tonoyan. Leveraging indirect signaling for topology inference and fast broadcast. In *Proceedings of the 2018 ACM Symposium on Principles of Distributed Computing, PODC '18*, pages 85–93, New York, NY, USA, 2018. ACM.
- [8] F. Ferrari, M. Zimmerling, L. Thiele, and O. Saukh. Efficient network flooding and time synchronization with glossy. In *Proceedings of the 10th ACM/IEEE International Conference on Information Processing in Sensor Networks*, pages 73–84, Chicago, IL, USA, April 2011. IEEE.
- [9] Birsen Sirkeci-Mergen, Anna Scaglione, and Gökhan Mergen. Asymptotic analysis of multistage cooperative broadcast in wireless networks. *IEEE/ACM Trans. Netw.*, 14(SI):2531–2550, June 2006.
- [10] Feng Xue and Panganamala R Kumar. The number of neighbors needed for connectivity of wireless networks. *Wireless networks*, 10(2):169–181, 2004.
- [11] Piyush Gupta and P. R. Kumar. The Capacity of Wireless Networks. *IEEE Transactions on Information Theory*, 46:388–404, 2000.
- [12] Chen Avin, Yuval Emek, Erez Kantor, Zvi Lotker, David Peleg, and Liam Roditty. SINR Diagrams: Convexity and Its Applications in Wireless Networks. *J. ACM*, 59(4):18, 2012.
- [13] Lun Dong, AP. Petropulu, and H.V. Poor. A cross-layer approach to collaborative beamforming for wireless ad hoc networks. *Signal Processing, IEEE Transactions on*, 56(7):2981–2993, July 2008.
- [14] Ayfer Özgür, Olivier Leveque, and David Tse. Hierarchical Cooperation Achieves Optimal Capacity Scaling in Ad Hoc Networks. *IEEE Transactions on Information Theory*, 53(10):3549–3572, October 2007.
- [15] Urs Niesen, Piyush Gupta, and Devavrat Shah. On Capacity Scaling in Arbitrary Wireless Networks. *IEEE Transactions on Information Theory*, 55(9):3959–3982, 2009.
- [16] Massimo Franceschetti, Marco Donald Migliore, and Paolo Minero. The capacity of wireless networks: Information-theoretic and physical limits. *IEEE Transactions on Information Theory*, 55(8):3413–3424, 2009.
- [17] Ayfer Özgür, Olivier Lévêque, and David Tse. Spatial degrees of freedom of large distributed mimo systems and wireless ad hoc networks. *IEEE Journal on Selected Areas in Communications*, 31(EPFL-ARTICLE-185421):202–214, 2013.
- [18] Ozgur Oyman and Arogyaswami J Paulraj. Power-bandwidth tradeoff in dense multi-antenna relay networks. *IEEE Transactions on Wireless Communications*, 6(6), 2007.
- [19] Ozgur Oyman and Arogyaswami J Paulraj. Cooperative OFDMA and distributed MIMO relaying over dense wireless networks, September 27 2011. US Patent 8,027,301.
- [20] Alla Merzakreeva, Ayfer Özgür, and Olivier Lévêque. Telescopic beamforming for large wireless networks. In *IEEE Int. Symposium on Information Theory*, Istanbul, 2013.
- [21] Thomas Janson and Christian Schindelhauer. Ad-Hoc Network Unicast in $\mathcal{O}(\log \log n)$ using Beamforming. <http://arxiv.org/abs/1405.0417>, May 2014.
- [22] Thomas Janson and Christian Schindelhauer. Broadcasting in Logarithmic Time for Ad Hoc Network Nodes on a Line using MIMO. In *Proceedings of the 25th ACM Symposium on Parallelism in Algorithms and Architectures, SPAA'13*. ACM, July 2013.

- [23] Thomas Janson. *Energy-Efficient Collaborative Beamforming in Wireless Ad Hoc Networks*. PhD thesis, University of Freiburg, Germany, 2015.
- [24] Thomas Janson and Christian Schindelhauer. Cooperative beamforming in ad-hoc networks with sublinear transmission power. In *IEEE 10th International Conference on Wireless and Mobile Computing, Networking and Communications (WiMob)*, pages 144–151, Larnaca, Cyprus, Oct 2014. IEEE.
- [25] Federico Ferrari, Marco Zimmerling, Luca Mottola, and Lothar Thiele. Low-power wireless bus. In *Proceedings of the 10th ACM Conference on Embedded Network Sensor Systems, SenSys '12*, pages 1–14, New York, NY, USA, 2012. ACM.
- [26] Felix Sutton, Bernhard Buchli, Jan Beutel, and Lothar Thiele. Zippy: On-demand network flooding. In *Proceedings of the 13th ACM Conference on Embedded Networked Sensor Systems*, pages 45–58. ACM, 2015.
- [27] Timo Kumberg, Christian Schindelhauer, and Leonhard Reindl. Exploiting concurrent wake-up transmissions using beat frequencies. *Sensors*, 17(8):1717, 2017.
- [28] Birsen Sirkeci-Mergen and Michael C Gastpar. On the broadcast capacity of wireless networks with cooperative relays. *IEEE Transactions on Information Theory*, 56(8):3847–3861, 2010.
- [29] Sang-Woon Jeon and Sae-Young Chung. Two-phase opportunistic broadcasting in large wireless networks. In *Information Theory, 2007. ISIT 2007. IEEE International Symposium on*, pages 2771–2775. IEEE, 2007.
- [30] Thomas Janson and Christian Schindelhauer. Analyzing Randomly Placed Multiple Antennas for MIMO Wireless Communication. In *Fifth International Workshop on Selected Topics in Mobile and Wireless Computing (IEEE STWiMob)*, Barcelona, 2012.
- [31] Ayfer Ozgur, Olivier Lévêque, and NC David. Hierarchical cooperation achieves optimal capacity scaling in ad hoc networks. *IEEE Transactions on information theory*, 53(10):3549–3572, 2007.
- [32] Aditya Oak. Analysis of a collaborative iterative miso broadcasting algorithm. Master’s thesis, University of Freiburg, George-Koehler-Allee 101, 79110 Freiburg, Germany, March 2018.
- [33] Timothy Hickey, Qun Ju, and Maarten H Van Emden. Interval arithmetic: From principles to implementation. *Journal of the ACM (JACM)*, 48(5):1038–1068, 2001.
- [34] Wassily Hoeffding. Probability inequalities for sums of bounded random variables. *Journal of the American statistical association*, 58(301):13–30, 1963.
- [35] Thomas Janson and Christian Schindelhauer. Self-Synchronized Cooperative Beamforming in Ad-Hoc Networks. In *16th International Symposium on Stabilization, Safety, and Security of Distributed Systems (SSS'14)*, Paderborn, Germany, September 2014.